EUROPEAN ORGANIZATION FOR NUCLEAR RESEARCH

Proposal to the ISOLDE and Neutron Time-of-Flight Committee

Investigation of the nucleon distribution on the surface of radioactive xenon nuclei using antiprotons

October 6, 2024

O. Aberle[1], T. Aumann[2], N. Azaryan[1], M. L. Bissell[1], O. Boine-Frankenheim[3], U. Bonnes[2], F. Butin[1], P. Chiggiato[1], H. De Gersem[3], R. De Oliveira[1], P.-Y. Duerinck[4], J. A. Ferreira Somoza[1], J. Fischer[2], R. Holz[1], G. Hupin[5], P. Indelicato[6], B. Jenniger[1], M. Kirschbaum[1], C. Klink[1,2], M. Kowalska[1], R. Lazauskas[4], S. Malbrunot-Ettenauer[7], W. F. O. Müller[3], L. Nies[1], A. Obertelli[2], N. Paul[6], L. Riik[3], R. Rinaldesi[1], D. Rossi[2], M. Schlaich[2], A. Schmidt[1], E. Siesling[1], F. Wienholtz[2], C. Xanthopoulou[2],

[1] *CERN, 1211 Geneva 23, Switzerland*

[2] *Institut für Kernphysik, Technische Universität Darmstadt, 64289 Darmstadt, Germany*

[3] *Institut für Teilchenbeschleunigung und elektromagnetische Felder, Technische Universität Darmstadt, 64289 Darmstadt, Germany*

[4] *Institut Pluridisciplinaire Hubert Curien, CNRS/IN2P3, Université de Strasbourg, France*

[5] *Université Paris-Saclay, CNRS/IN2P3, IJCLab, 91405 Orsay, France*

[6] *Laboratoire Kastler Brossel, Sorbonne Université, CNRS, ENS-PSL Research University, Collège de France, France*

[7] *TRIUMF, Vancouver, Canada*

Spokespersons: L. Nies (lukas.nies@cern.ch),
F. Wienholtz (fwienholtz@ikp.tu-darmstadt.de)
Contact person: L. Nies (lukas.nies@cern.ch)

CERN-INTC-2024-055 / INTC-P-712
06/10/2024

Abstract:

We propose to measure the neutron-to-proton annihilation ratio of captured antiprotons in antiprotonic $^{115-144}$Xe atoms within the density tail of the nuclear matter distribution with a targeted precision of better than 10% to extract a quantitative understanding of how the increasing number of neutrons in the isotopic chain changes the nuclear density close to the nucleus' surface. For this, we will use the PUMA apparatus, transporting antiprotons created at the Antiproton Decelerator (AD) at CERN to the ISOLDE facility using a transportable Penning trap. The measurements will be performed at ISOLDE within the apparatus' Penning trap, in which the different radioactive and stable xenon nuclei will be mixed with a subcloud of the stored antiprotons. Pions created during the annihilation reaction are detected and identified using a time-projection chamber surrounding the Penning trap. The results will complement data previously taken at the AD using stable xenon isotopes with radioactive neutron-rich and deficient xenon isotopes, extending from the nine stable isotopes to a

total of 29 different xenon isotopes. In addition to providing new insights into how the surface density changes for different degrees of deformation in the xenon isotopic chain and the possible formation of neutron skins along it, our proposal constitutes the first experiment using antiprotons to investigate the nuclear structure of short-lived radioactive nuclei.

Requested shifts: 18 shifts in one run using a UC_x target together with a VD7 plasma ion source for the first part and 18 shifts using a LaC_x target together with a VD7 plasma ion source for the second run

1 Motivation

The PUMA (antiProton Unstable Matter Annihilation) apparatus is a nuclear physics experiment at CERN that uses low-energy antiprotons to probe the surface properties of stable and unstable isotopes. In 2021, the Super Proton Synchrotron Experiments Committee at CERN reviewed a new experimental proposal [1] and positively evaluated the PUMA apparatus as a new CERN experiment. Since then, significant milestones have been achieved towards the first antiproton annihilations with stable matter at CERN's antimatter decelerator (AD). In this manuscript, we propose the first experiment extending the measurements from stable xenon isotopes to unstable xenon nuclei provided by ISOLDE.

Historically, low-energy antiprotons were first used to probe the neutron-proton annihilation ratio on stable nuclei some five decades ago at Brookhaven National Laboratory, where in the case of ^{208}Pb, a factor of 2.3(5) more neutron annihilations were observed compared to the N/Z ratio one might expect [2]. Such excess in annihilation rate can be linked to neutron skins and halos. In particular, the neutron skin in ^{208}Pb has been extensively studied through electroweak [3], hardronic [4, 5], electromagnetic [6], and astronomical probes [7]. Notably, modern nuclear *ab initio* theory has been proven to reproduce this observable on a microscopic level, linking the neutron skin thickness directly to nuclear forces [8].

Several of these works have extracted the neutron skin thickness of stable nuclei in a model-dependent way. In contrast, PUMA aims to characterize the tail of the nuclear density of radioactive nuclei by measuring low-energy annihilation products. Our proposed experiment offers a new technique with a unique sensitivity for studying the neutron-to-proton density in the tail of the nucleus's density distribution in the order of one or two femtometers away from the nucleon surface. This technique complements the commonly used nucleon knockout reaction (see left diagram in Fig. 1), which takes place at high beam energies directly on the surface of the nucleus, thus providing a new and unexplored observable to constrain nuclear theory.

Extending this technique to radioactive ions was first proposed by Wada and Yamazaki [9]. However, to date, no existing facility combines the possibility of performing experiments with antiprotons and radioactive ions at low energy. To combine the two and utilize both capabilities, antiprotons must be transported to a radioactive ion beam facility if short-lived isotopes are to be considered for experiments. The PUMA transportable Penning trap [10] will fill this gap and thus allow the transport of antiprotons from the AD to the ISOLDE facility.

Due to several reasons, xenon isotopes were selected as the first element to perform experiments with antiprotons at ISOLDE. Firstly, the nine stable xenon isotopes will be investigated in the PUMA apparatus using the offline ion source of PUMA at the AD (only gases are available so far) in preparation for the ISOLDE experiment. These results are necessary for benchmarking the data taken at the two different facilities and for characterizing any environment-dependent systematics. In contrast to the offline work at the AD, about 29 different xenon isotopes, including the stable ones, can be delivered by ISOLDE with sufficient intensity $\left(>5\times10^{5}\mu C^{-1}\right)$ as isobarically pure beams. Isobaric purity in the order of better than 99% is paramount to achieve relative accuracies of better than 2% in the n/p annihilation ratio signal.

Secondly, with a proton number of $Z = 54$, xenon exhibits a large number of electrons

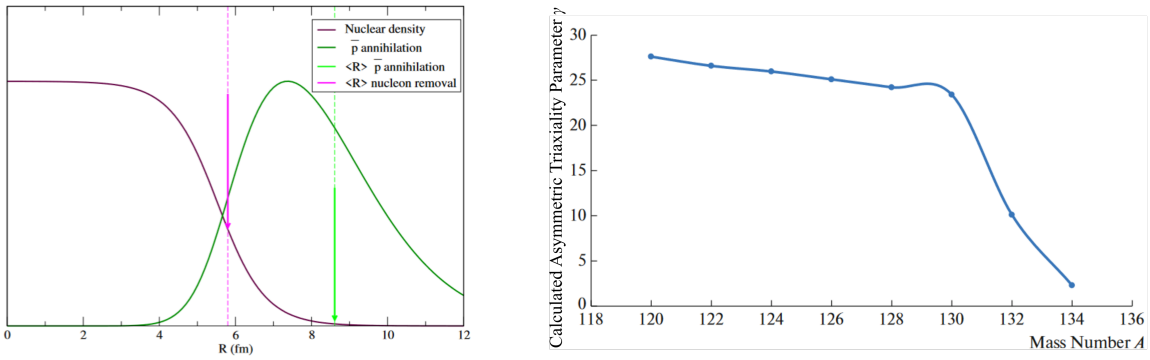

Figure 1: Left: Nuclear density as a function of the radius of including the annihilation probability and the expected radial positions to which the nucleon removal at high beam energy and the antiproton annihilation techniques are sensitive to [10]. Right: The calculated asymmetry triaxiality parameter γ as a function of mass number A for different Xenon isotopes [15]

orbiting the nucleus, which leads to an increased antiproton capture cross section at low energies.

Third, neutron skins could be characterized by a n/p annihilation ratio larger than the nucleonic ratio N/Z. It has been shown in Ref. [11] through calculation of the ratio of the absorption widths for protons and neutrons for different Skyrme parameterizations that for calcium and tin isotopes, the PUMA method is sensitive to small ($\pm$0.1 fm) variations of the neutron skin thickness [11], suggesting similar sensitivity to the xenon isotopic chain.

The *nucleonic ratio* N/P in the selected isotopes ranges from 1.15 (^{116}Xe) over 1.48 (^{132}Xe) to 1.67 (^{144}Xe). The *n/p matter density ratio*, i.e. the matter density of neutrons and protons on the surface of the nucleus, is expected to range from 1.2 (^{116}Xe) over 2.1 (^{132}Xe) to 3.3 (^{144}Xe). Our observable, the *n/p annihilation ratio*, however, is expected to be closer to 0.7 (^{116}Xe), 1.3 (^{132}Xe), and 2.1 (^{144}Xe), taking into account that the annihilation cross-section of antiprotons with protons is slightly larger than with neutron [2, 12, 13, 14].

Furthermore, the xenon isotopic chain is predicted to show a significant variation of the asymmetric triaxiality parameter γ, which represents the degree of triaxial deformation along its isotope chain [15] (see the right diagram of Fig. 1) which raises the question if this effect can also be seen in a change of the n/p annihilation ratio due to a deformation-driven change of the surface density of the nucleus. Triaxiality has to be considered for the formation of halo nuclei [16], which are the focus of future experiments with PUMA; thus, showing sensitivity to this parameter would pave the way to future measurements. Xenon will thus be an ideal test bench to test the general operation procedure that the PUMA experiment will experience in the future to perform more experiments with radioactive beams and antiprotons at ISOLDE.

2 Experimental techniques

The PUMA experiment uses antiprotons to study the annihilation reactions with surface nucleons of stable and radioactive ions. For this, antiprotons delivered at a beam energy of 100 keV by the ELENA synchrotron [17] are accumulated in a Penning trap at the antimatter decelerator at CERN. To capture the bunched antiprotons of about $\approx 5 \times 10^6$ antiprotons per pulse, the bunch has to be further decelerated to about 4 keV using a high voltage pulsed drift tube [18, 19] of the PUMA experiment at the LNE51 beamline. A deceleration efficiency of 60% was demonstrated. The antiproton bunch is then ion-optically guided to the PUMA Penning traps [20] within the transportable frame of the experiment. An overview of the setup at LNE51 can be seen in Fig. 2.

The Penning trap tower consists of two Penning traps, which can be used to accumulate and store the antiproton cloud as well as a region in which the antiprotons are mixed with the different isotopes, called the measurement Penning trap [20, 10]. This area is additionally surrounded (outside the vacuum tube) by a time-projection chamber (TPC) [11], which enables the detection of the annihilation products. A cross-sectional view of the CAD representation of the Penning trap tower and the surrounding equipment can be seen in Fig. 3. A certain number of antiprotons can be transferred from the storage Penning trap into the measurement Penning trap. At the same time, ions of interest provided by and offline source at the AD or by the ISOL method at ISOLDE accumulate directly in the measurement Penning trap. Different mixing schemes [20] will then be applied until the antiprotons are captured by the ions, forming antiprotonic atoms, followed by subsequent annihilations (see left Fig. 4).

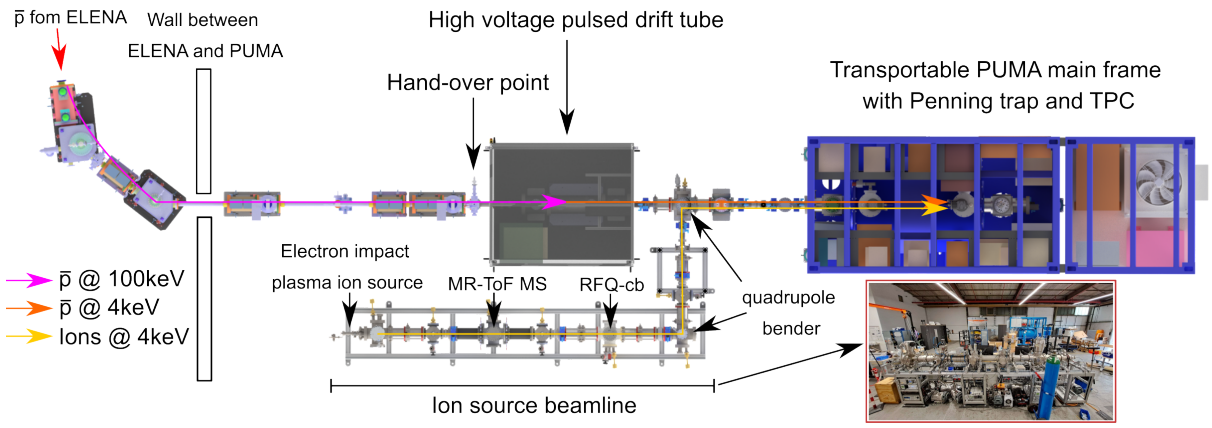

Figure 2: Representation of the PUMA setup at the LNE51 beamline at the AD. The main components are the high-voltage pulsed drift tube, the transportable PUMA main frame with the Penning trap, the TPC, and all necessary supporting equipment, as well as the ion source arrangement shown in the included picture.

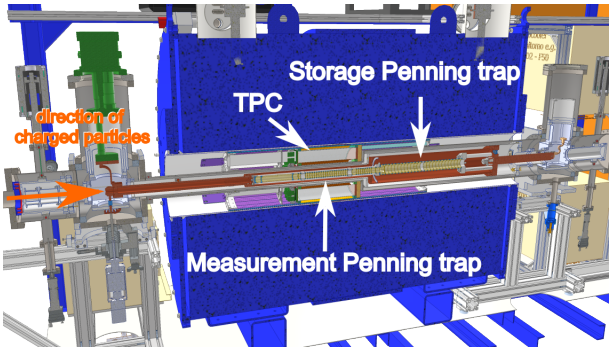

Figure 3: Cross-sectional view of the CAD model of the PUMA frame. The main components are the measurement and the storage Penning trap, as well as the TPC marked in the picture. The direction in which the charged particles are introduced is marked in orange

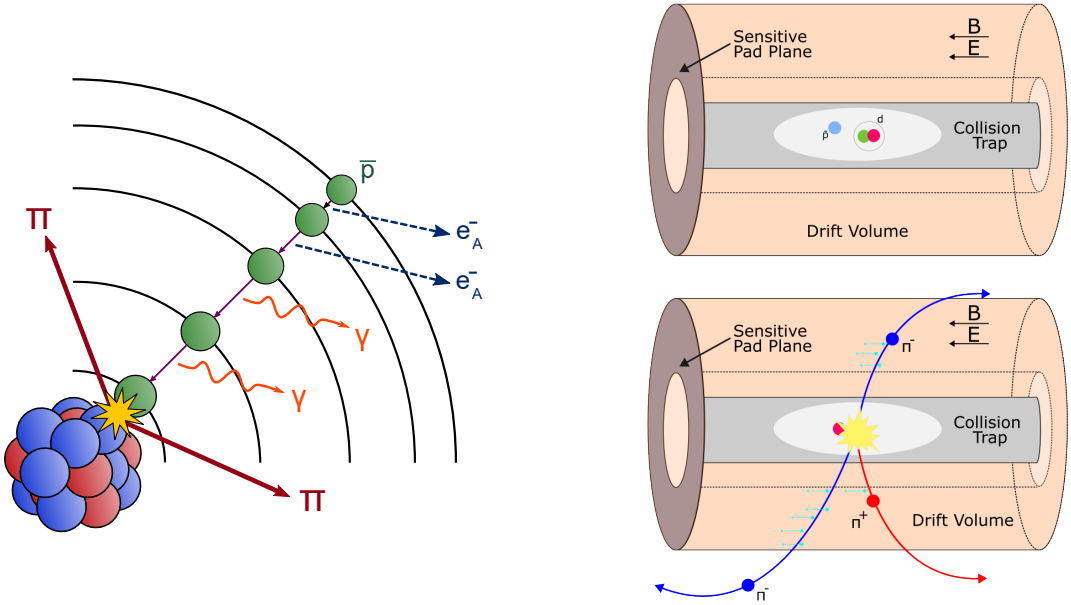

Figure 4: Left: Illustration of the formation process of an antiprotonic atom including the cascade of the antiproton towards the nucleus while emitting Auger electrons and electromagnetic radiation until the annihilation with a nucleon followed by pion emission. Right: Illustration of the TPC working principle surrounding the collision Penning trap, which enables the detection and identification of pions.

The pions emitted in the annihilation reaction can be detected and identified with the TPC. The TPC can detect and correctly identify the charge for 77.5% of all pions that are emitted [11]. Furthermore, a trigger barrel made of scintillator bars equipped with silicon photomultipliers surrounds the TPC and extends over both Penning traps to provide a start trigger for the measurements and to suppress detector background due to cosmic radiation. A trigger efficiency of about 70% with respect to the emitted pions is expected, together with a time resolution of 1 ns using a silicon photomultiplier readout. It can also be used to monitor the rate of annihilations that the antiprotons experience either during the measurement or the transport and storage.

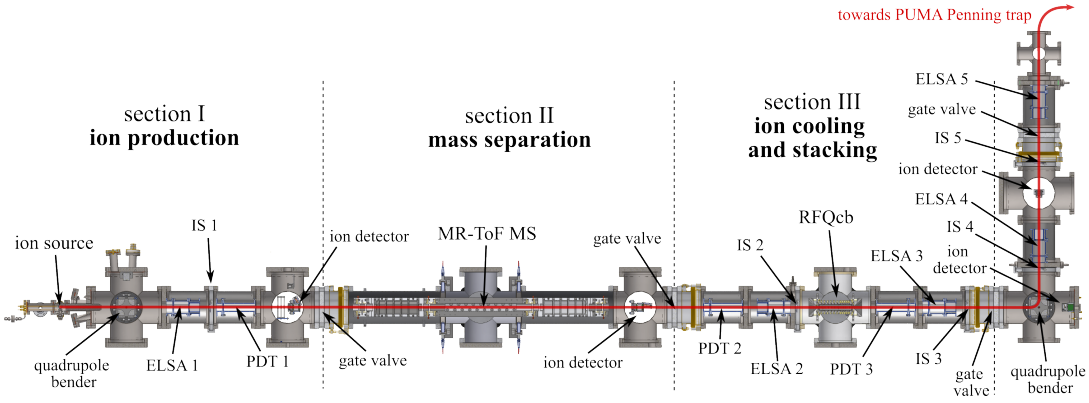

Figure 5: Top half-section view onto the offline ion source beamline of the PUMA experiment at the AD, which consists of four sections: ion production, mass separation, ion cooling, and stacking and transfer to the Puma Penning traps. The beamline includes an einzel lens and steerer assemblies (ELSA), pulsed drift tubes (PDT), and iris shutter apertures (IS).

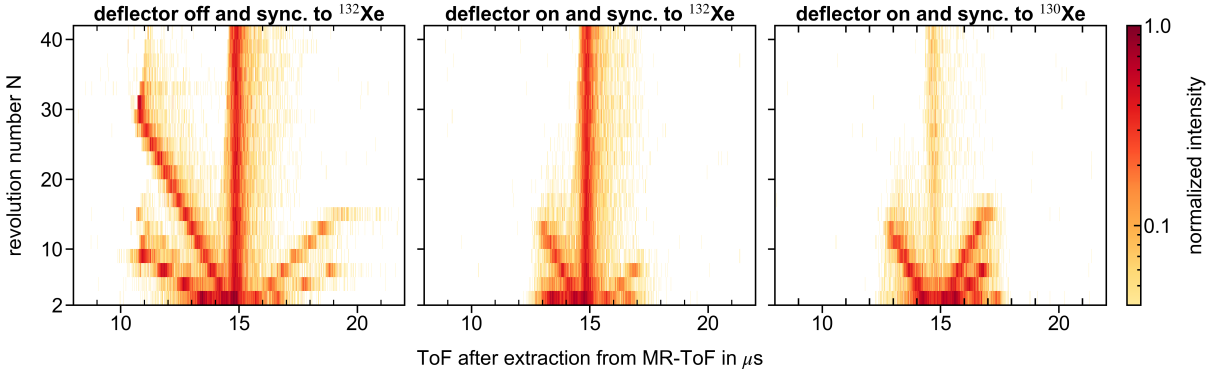

Figure 6: Time-of-flight spectra for different number of revolutions in the MR-ToF MS focussing on ^{132}Xe.

The pions created in the center of the measurement Penning trap fly through the gaseous volume of the TPC and ionize the gas, creating free electrons. These electrons are accelerated towards the segmented pad plane equipped with an amplification stage. This allows for the reconstruction of the track of the pions flying through the TPC. Due to the strong magnetic field of the PUMA solenoid, the pion tracks are curved according to the charge of the pions. This finally allows to distinguish between the different species and to count them accordingly.

The first experiments will be performed at the AD itself, using the ion source setup presented in Fig. 5 and described in more detail in [21]. It currently allows the production, separation, cooling, and accumulation of ions from different noble gases. Xenon gas with naturally distributed abundance is used to generate pure, cooled bunches of all (quasi-)stable xenon isotopes (A=124, 125, 128-132, 134, 136).

To achieve this, the deflector technique [22] developed for multi-reflection time-of-flight mass separators (MR-ToF MS) is employed within the newly developed MR-ToF MS [21] for the ion source of PUMA. It allows unwanted ions to be removed with a high mass

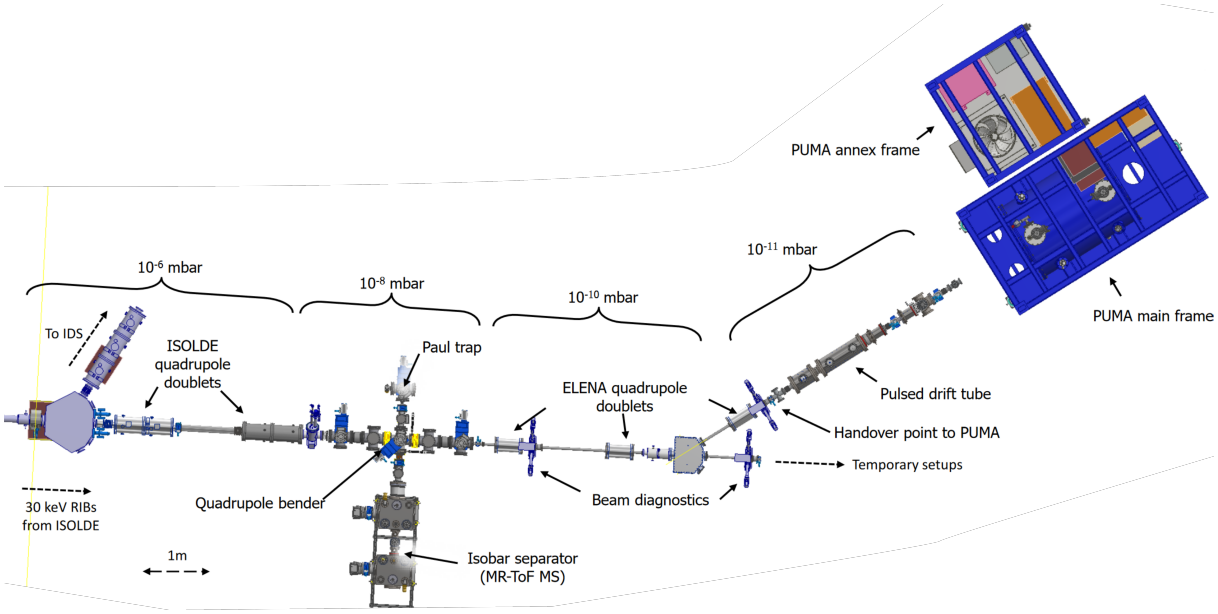

Figure 7: The PUMA experiment will be situated at the newly installed RC6-RC7 beamline in the hall extension of ISOLDE, neighbouring the Miniball experiment. Within the responsibility of the PUMA collaboration is the equipment after the handover point (RC7 part), which accommodates an additional pulsed drift tube, ion optics, and diagnostics for the injection into the PUMA Penning traps.

separation power and a high suppression factor. Within the ion source section of PUMA, a radiofrequency quadrupole cooler-buncher (RFQ-cb) allows the mass-separated beam to be cooled and accumulated. It was demonstrated that ^{126}Xe, with 0.089% by far the lowest abundant isotope in the xenon chain, could be accumulated to $\approx 10^3$ pure ions per bunch in the RFQ-cb in less than one second (further accumulation possible) while bunches of several 10^5 ions per bunch can be captured for ^{132}Xe (26.9% abundance) in the same time. The data collected on the nine stable xenon isotopes is perfectly suited for characterizing and comparing the experiment's performance before the actual transport to ISOLDE.

Before the transportable frame can then be disconnected from the beamline, craned onto a truck, and transported to ISOLDE, where it is again transported by crane into the foreseen position at the RC6-RC7 low-energy beamline, about 10^8 antiprotons have to be accumulated in PUMA to be transported per experimental run at ISOLDE. Ultimately, the PUMA collaboration aims to transport 10^9 antiprotons inside the storage Penning trap. An overview of the RC6-RC7 beamline is shown in Fig. 7

3 Beam time request

As mentioned previously, the xenon isotopic chain has been selected due to its large range of stable and unstable isotopes available at ISOLDE at high rates and in high beam purity. The latter is achieved by operating the target in combination with the VD7 cold plasma ion source, which operates the transfer line at room temperature. This effectively freezes out

most species produced in the target and transmits only volatile atoms and molecules at these relatively low temperatures, such as noble gases and other gaseous molecules.

One of the ISOLDE mass separators delivers the ion beam from the VD7 through the central beamline into the RC beamline, where the new RC6 transfer beamline is currently being constructed. For this experiment, the high-energy isobar separator at RC6 will not be needed as the xenon beam purity allows for direct processing in either the ISCOOL RFQ-cb or the RC6 RFQ-cb. If the RC6 RFQ-cb is already available at the time of the experiment, the GPS front end can be used. Otherwise, HRS in combination with ISCOOL will be required (note that the temporal length of the ion bunch delivered by either of the two RFQ-cb has to be much smaller than 1 µs to be efficiently captured by the PUMA apparatus).

A pulsed drift tube slows down the pulsed beam arriving at the RC7 beamline of PUMA with 30 keV energy to 4 keV beam energy, similar to the setup at the AD for the deceleration of the antiprotons. Ion-optical elements allow the injection into the PUMA Penning traps, and the same experimental cycle is performed as described before for the operation of PUMA at the AD.

A detailed description of the requested beams, together with a breakdown of the requested shifts, can be found in Appendix A.2 and A.3. The number of requested shifts builds on rate estimates based on low-energy antiproton-ion annihilation cross-sections, nuclear half-lives, detector efficiencies, and data analysis methods detailed in Appendix A.4.

We summarize the requested protons: 18 shifts in one run using a UC_x target together with a VD7 plasma ion source for the first part and 18 shifts using a LaC_x target together with a VD7 plasma ion source for the second run.

References

[1] T Aumann, W Bartmann, A Bouvard, O Boine-Frankenheim, A Broche, F Butin, D Calvet, J Carbonell, P Chiggiato, H De Gersem, R De Oliveira, T Dobers, F Ehm, J Ferreira Somoza, J Fischer, M Fraser, E Friedrich, J-L Grenard, G Hupin, K Johnston, Y Kubota, M Gomez-Ramos, P Indelicato, R Lazauskas, S Malbrunot-Ettenauer, N Marsic, W Müller, S Naimi, N Nakatsuka, R Necca, G Neyens, A Obertelli, Y Ono, S Pasinelli, N Paul, E C Pollacco, D Rossi, H Scheit, R Seki, A Schmidt, L Schweikhard, S Sels, E Siesling, T Uesaka, M Wada, F Wienholtz, S Wycech, and S Zacarias. PUMA: antiprotons and radioactive nuclei. Technical report, CERN, Geneva, 2019.

[2] W. M. Bugg, G. T. Condo, E. L. Hart, H. O. Cohn, and R. D. McCulloch. Evidence for a neutron halo in heavy nuclei from antiproton absorption. *Phys. Rev. Lett.*, 31:475–478, Aug 1973.

[3] D. Adhikari, H. Albataineh, D. Androic, K. Aniol, D. S. Armstrong, T. Averett, C. Ayerbe Gayoso, S. Barcus, V. Bellini, R. S. Beminiwattha, J. F. Benesch, H. Bhatt, D. Bhatta Pathak, D. Bhetuwal, B. Blaikie, Q. Campagna, A. Camsonne, G. D. Cates, Y. Chen, C. Clarke, J. C. Cornejo, S. Covrig Dusa, P. Datta, A. Deshpande, D. Dutta, C. Feldman, E. Fuchey, C. Gal, D. Gaskell, T. Gautam, M. Gericke, C. Ghosh, I. Halilovic, J.-O. Hansen, F. Hauenstein, W. Henry, C. J. Horowitz, C. Jantzi, S. Jian, S. Johnston, D. C. Jones, B. Karki, S. Katugampola, C. Keppel, P. M. King, D. E. King, M. Knauss, K. S. Kumar, T. Kutz, N. Lashley-Colthirst, G. Leverick, H. Liu, N. Liyange, S. Malace, R. Mammei,

J. Mammei, M. McCaughan, D. McNulty, D. Meekins, C. Metts, R. Michaels, M. M. Mondal, J. Napolitano, A. Narayan, D. Nikolaev, M. N. H. Rashad, V. Owen, C. Palatchi, J. Pan, B. Pandey, S. Park, K. D. Paschke, M. Petrusky, M. L. Pitt, S. Premathilake, A. J. R. Puckett, B. Quinn, R. Radloff, S. Rahman, A. Rathnayake, B. T. Reed, P. E. Reimer, R. Richards, S. Riordan, Y. Roblin, S. Seeds, A. Shahinyan, P. Souder, L. Tang, M. Thiel, Y. Tian, G. M. Urciuoli, E. W. Wertz, B. Wojtsekhowski, B. Yale, T. Ye, A. Yoon, A. Zec, W. Zhang, J. Zhang, and X. Zheng. Accurate determination of the neutron skin thickness of ^{208}Pb through parity-violation in electron scattering. *Phys. Rev. Lett.*, 126:172502, Apr 2021.

[4] A. Trzcińska, J. Jastrzębski, P. Lubiński, F. J. Hartmann, R. Schmidt, T. von Egidy, and B. Kłos. Neutron density distributions deduced from antiprotonic atoms. *Phys. Rev. Lett.*, 87:082501, Aug 2001.

[5] J. Zenihiro, H. Sakaguchi, T. Murakami, M. Yosoi, Y. Yasuda, S. Terashima, Y. Iwao, H. Takeda, M. Itoh, H. P. Yoshida, and M. Uchida. Neutron density distributions of ^{204,206,208}Pb deduced via proton elastic scattering at E_p = 295 mev. *Phys. Rev. C*, 82:044611, Oct 2010.

[6] C. M. Tarbert, D. P. Watts, D. I. Glazier, P. Aguar, J. Ahrens, J. R. M. Annand, H. J. Arends, R. Beck, V. Bekrenev, B. Boillat, A. Braghieri, D. Branford, W. J. Briscoe, J. Brudvik, S. Cherepnya, R. Codling, E. J. Downie, K. Foehl, P. Grabmayr, R. Gregor, E. Heid, D. Hornidge, O. Jahn, V. L. Kashevarov, A. Knezevic, R. Kondratiev, M. Korolija, M. Kotulla, D. Krambrich, B. Krusche, M. Lang, V. Lisin, K. Livingston, S. Lugert, I. J. D. MacGregor, D. M. Manley, M. Martinez, J. C. McGeorge, D. Mekterovic, V. Metag, B. M. K. Nefkens, A. Nikolaev, R. Novotny, R. O. Owens, P. Pedroni, A. Polonski, S. N. Prakhov, J. W. Price, G. Rosner, M. Rost, T. Rostomyan, S. Schadmand, S. Schumann, D. Sober, A. Starostin, I. Supek, A. Thomas, M. Unverzagt, Th. Walcher, L. Zana, and F. Zehr. Neutron skin of ^{208}Pb from coherent pion photoproduction. *Phys. Rev. Lett.*, 112:242502, Jun 2014.

[7] F. J. Fattoyev, J. Piekarewicz, and C. J. Horowitz. Neutron skins and neutron stars in the multimessenger era. *Phys. Rev. Lett.*, 120:172702, Apr 2018.

[8] Baishan Hu, Weiguang Jiang, Takayuki Miyagi, Zhonghao Sun, Andreas Ekström, Christian Forssén, Gaute Hagen, Jason D. Holt, Thomas Papenbrock, S. Ragnar Stroberg, and Ian Vernon. Ab initio predictions link the neutron skin of 208pb to nuclear forces. *Nature Physics*, 18(10):1196–1200, Oct 2022.

[9] Michiharu Wada and Yasunori Yamazaki. Technical developments toward antiprotonic atoms for nuclear structure studies of radioactive nuclei. *Nuclear Instruments and Methods in Physics Research Section B: Beam Interactions with Materials and Atoms*, 214:196–200, 2004. Low Energy Antiproton Physics (LEAP'03).

[10] T. Aumann, W. Bartmann, O. Boine-Frankenheim, A. Bouvard, A. Broche, F. Butin, D. Calvet, J. Carbonell, P. Chiggiato, H. De Gersem, R. De Oliveira, T. Dobers, F. Ehm, J. Ferreira Somoza, J. Fischer, M. Fraser, E. Friedrich, A. Frotscher, M. Gomez-Ramos, J.-L. Grenard, A. Hobl, G. Hupin, A. Husson, P. Indelicato, K. Johnston, C. Klink, Y. Kubota, R. Lazauskas, S. Malbrunot-Ettenauer, N. Marsic, W. F. O Müller, S. Naimi, N. Nakatsuka, R. Necca, D. Neidherr, G. Neyens, A. Obertelli, Y. Ono, S. Pasinelli, N. Paul, E. C. Pollacco, D. Rossi, H. Scheit, M. Schlaich, A. Schmidt, L. Schweikhard, R. Seki, S. Sels, E. Siesling,

T. Uesaka, M. Vilén, M. Wada, F. Wienholtz, S. Wycech, and S. Zacarias. PUMA, antiProton unstable matter annihilation. *European Physical Journal A*, 58:88, 05 2022.

[11] Sabrina Zacarias. *Probing nuclear density tails with antiprotons at PUMA: Detection and method*. PhD thesis, Technische Universität Darmstadt, Darmstadt, 2022.

[12] W. Chinowsky and G. Kojoian. Antiproton annihilation at rest in deuterium. *Il Nuovo Cimento A (1965-1970)*, 43(3):684–700, Jun 1966.

[13] M. Wade and V. G. Lind. Ratio of antiproton annihilations on neutrons and protons in carbon for low-energy and stopped antiprotons. *Phys. Rev. D*, 14:1182–1187, Sep 1976.

[14] J. Riedlberger, C. Amsler, M. Doser, U. Straumann, P. Truöl, D. Bailey, S. Barlag, U. Gastaldi, R. Landua, C. Sabev, K. D. Duch, M. Heel, H. Kalinowsky, F. Kayser, E. Klempt, B. May, O. Schreiber, P. Weidenauer, M. Ziegler, W. Dahme, F. Feld-Dahme, U. Schaefer, W. R. Wodrich, S. Ahmad, J. C. Bizot, B. Delcourt, J. Jeanjean, H. Nguyen, N. Prevot, E. G. Auld, D. A. Axen, K. L. Erdman, B. Howard, R. Howard, B. L. White, M. Comyn, G. Beer, G. M. Marshall, L. P. Robertson, M. Botlo, C. Laa, and H. Vonach. Antiproton annihilation at rest in nitrogen and deuterium gas. *Phys. Rev. C*, 40:2717–2731, Dec 1989.

[15] W. B. Elsharkawy, Abeer Mera, M. Kotb, and A. M. Khalaf. Nuclear shape transition, triaxiality and energy staggering of γ-band states for even–even xenon isotopic chain. *Physics of Atomic Nuclei*, 2023.

[16] K. Uzawa, K. Hagino, and K. Yoshida. Role of triaxiality in deformed halo nuclei. *Phys. Rev. C*, 104:L011303, Jul 2021.

[17] Vinod Chohan, C Alanzeau, M E Angoletta, J Baillie, D Barna, W Bartmann, P Belochitskii, J Borburgh, H Breuker, F Butin, M Buzio, O Capatina, C Carli, E Carlier, M Cattin, T Dobers, P Chiggiato, L Ducimetiere, T Eriksson, S Fedemann, T Fowler, R Froeschl, R Gebel, N Gilbert, S Hancock, J Harasimowicz, M Hori, L V Jorgensen, R Kersevan, D Kuchler, J M Lacroix, G LeGodec, P Lelong, L Lopez-Hernandez, S Maury, J Molendijk, B Morand, A Newborough, D Nisbet, A Nosych, W Oelert, M Paoluzzi, S Pasinelli, F Pedersen, D Perini, B Puccio, J Sanchez-Quesada, D Schoerling, L Sermeus, L Soby, M Timmins, D Tommasini, G Tranquille, G Vanbavinckhove, A Vorozhtsov, C Welsch, and T Zickler. *Extra Low ENergy Antiproton (ELENA) ring and its Transfer Lines: Design Report*. CERN Yellow Reports: Monographs. CERN, Geneva, 2014.

[18] Jonas Fischer, Alexander Schmidt, Nikolay Azaryan, François Butin, Jose Ferreira Somoza, Audric Husson, Clara Klink, Alexandre Obertelli, Moritz Schlaich, Alexandre Sinturel, Nicolas Thaus, and Frank Wienholtz. Design and characterization of an antiproton deceleration beamline for the puma experiment. *Nuclear Instruments and Methods in Physics Research Section B: Beam Interactions with Materials and Atoms*, 550:165318, 2024.

[19] Jonas Ludwig Fischer. *Deceleration of Antiprotons for High-Efficiency Accumulation at PUMA*. PhD thesis, Technische Universität Darmstadt, Darmstadt, Mai 2024.

[20] Alexander Schmidt. *Development of the PUMA Antiproton and Ion Trap*. PhD thesis, Technische Universität Darmstadt, Darmstadt, Januar 2024.

[21] M. Schlaich, J. Fischer, P. Fischer, C. Klink, A. Obertelli, A. Schmidt, L. Schweikhard, and F. Wienholtz. A multi-reflection time-of-flight mass spectrometer for the offline ion source of the puma experiment. *International Journal of Mass Spectrometry*, 495:117166, 2024.

[22] Paul Fischer, Stefan Knauer, Gerrit Marx, and Lutz Schweikhard. In-depth study of in-trap high-resolution mass separation by transversal ion ejection from a multi-reflection time-of-flight device. *Review of Scientific Instruments*, 89:015114, 2018.

[23] R.N. Wolf et al. ISOLTRAP's multi-reflection time-of-flight mass separator/spectrometer. *International Journal of Mass Spectrometry*, 349-350:123, 2013.

[24] Eoin Butler. *Antihydrogen formation, dynamics and trapping*. PhD thesis, Swansea U., Swansea U., 2011.

[25] James S. Cohen. Capture of antiprotons by some radioactive atoms and ions. *Phys. Rev. A*, 69:022501, Feb 2004.

[26] P. Delahaye, F. Ames, and A. Kellerbauer. Study of the charge exchange process at low energy with rextrap. *Nuclear Physics A*, 746:604–607, 2004. Proceedings of the Sixth International Conference on Radioactive Nuclear Beams (RNB6).

A Details for the Technical Advisory Committee

A.1 General information

The PUMA setup will be used in this experiment. As PUMA is transporting antimatter from CERN-AD to CERN-ISOLDE, only a short transfer beamline located at the new low-energy beamline RC7 is permanently installed. This permanent installation, which serves as the interface between ISOLDE and PUMA, includes a pulsed drift tube to reduce the incoming ion beam energy to be captured in the PUMA experiment and a diagnostics station.

☒ Permanent ISOLDE setup: PUMA

- ☒ To be used without modification
- ☐ To be modified: /

A.2 Beam production

For this experiment, we propose to use two different target materials to reach the neutron-deficient and neutron-rich xenon isotopes. The following table shows isotope properties and a detailed summary of the shift request. The experiment requires at least 10^5 ions per 2.4 s delivered to the annihilation region.

Isotope	Half-Life	Yield in CA0 (1/uC)	Target / Ion source	Protons	Shifts (8h)
^{115}Xe	18.0 s	6.7×10^5	LaC_x / VD7	Yes	1
^{116}Xe	59.0 s	6.5×10^6	LaC_x / VD7	Yes	1
^{117}Xe	61.0 s	5.0×10^7	LaC_x / VD7	Yes	0.5
^{118}Xe	3.8 min	5.9×10^7	LaC_x / VD7	Yes	0.5
^{119}Xe	5.8 min	7.1×10^7	LaC_x / VD7	Yes	0.5
^{120}Xe	46.0 min	1.6×10^8	LaC_x / VD7	Yes	0.5
^{121}Xe	40.1 min	$> 1.0 \times 10^8$	LaC_x / VD7	Yes	0.5
^{122}Xe	20.1 h	$> 1.0 \times 10^8$	LaC_x / VD7	Yes	0.5
^{123}Xe	2.08 h	$> 1.0 \times 10^8$	LaC_x / VD7	Yes	0.5
^{124}Xe	stable	/	LaC_x / VD7	No	0.5
^{125}Xe	16.87 h	4.7×10^8	LaC_x / VD7	Yes	0.5
^{126}Xe	stable	/	LaC_x / VD7	No	0.5
^{127}Xe	36.342 d	5.2×10^8	LaC_x / VD7	Yes	0.5
^{128}Xe	stable	/	UC_x / VD7	No	0.5
^{129}Xe	stable	/	UC_x / VD7	No	0.5
^{130}Xe	stable	/	UC_x / VD7	No	0.5
^{131}Xe	stable	/	UC_x / VD7	No	0.5
^{132}Xe	stable	/	UC_x / VD7	No	0.5
^{133}Xe	5.25 d	$> 6.0 \times 10^8$	UC_x / VD7	Yes	0.5
^{134}Xe	stable	/	UC_x / VD7	No	0.5
^{135}Xe	9.14 h	$> 6.0 \times 10^8$	UC_x / VD7	Yes	0.5
^{136}Xe	2.18 Zy	$> 6.0 \times 10^8$	UC_x / VD7	No	0.5

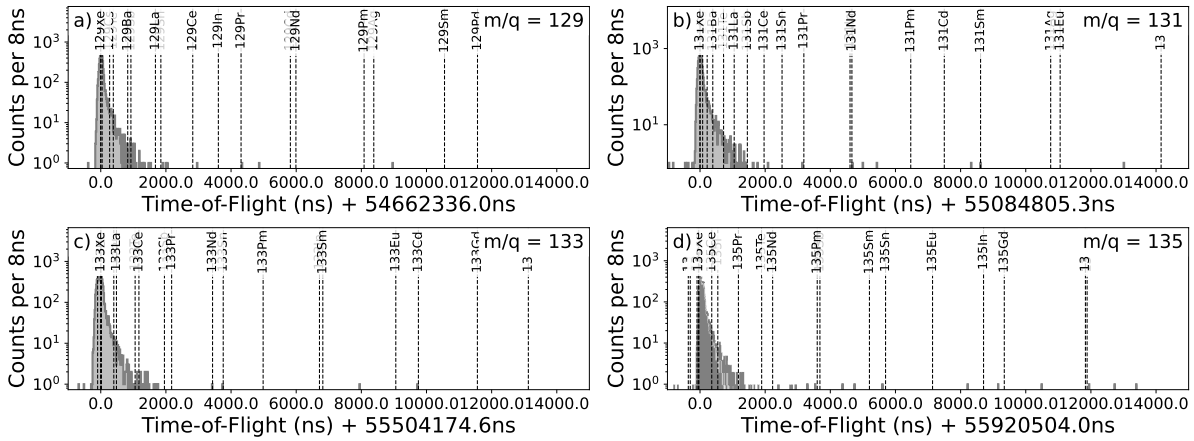

Figure 8: Time-of-flight spectra using ISOLTRAP to investigate beam purity of radioactive xenon ion beams near stability from target #760-VD7 in July 2023.

^{137}Xe	3.8 min	6.2×10^8	UC_x / VD7	Yes	0.5
^{138}Xe	14.14 min	5.7×10^8	UC_x / VD7	Yes	0.5
^{139}Xe	39.68 s	5.0×10^8	UC_x / VD7	Yes	0.5
^{140}Xe	13.6 s	3.5×10^8	UC_x / VD7	Yes	0.5
^{141}Xe	1.73 s	5.9×10^7	UC_x / VD7	Yes	0.5
^{142}Xe	1.23 s	3.7×10^7	UC_x / VD7	Yes	1
^{143}Xe	511 ms	6.6×10^6	UC_x / VD7	Yes	1
^{144}Xe	388 ms	9.9×10^5	UC_x / VD7	Yes	1

The yields were extracted from the ISOLDE yield database in September 2024. To achieve cross-checks using stable xenon isotopes for comparisons with offline measurements performed at CERN-AD, the VD7 has to be operated using a noble gas mixture, including natural xenon gas, to provide the references. Furthermore, beam purity for the experiment is paramount. For this reason, the plasma source's transfer line must be operated cold, i.e., at room temperature. During xenon collections in July 2023 from target #760 (UC_x-VD7) on GPS, no isobaric contamination was observed, confirmed through multi-reflection time-of-flight mass spectrometry. At the time of measurement, the target temperature was 1900 °C (600 A).

Figure 8 shows the collected ToF spectra using the ISOLTRAP MR-ToF MS [23] during the test on target #760. As one can see, on the odd xenon masses $A = 129 - 135$, only xenon and it's long-lived isomeric states are present in the beam delivered by GPS (on $m/q = 133$, ^{133}Cs from the ISOLTRAP offline ion source is present in the spectrum for calibration purposes). In none of the beams surface-ionized cesium or barium was present.

A.3 Shift breakdown

Since neutron-deficient and neutron-rich xenon isotopes are to be delivered, two target units must be used, ideally on HRS if the RC6 RFQ-cb is not yet available; otherwise, on GPS. This

will require two separate experimental runs, giving the PUMA experiment time to return to the AD and recharge the antiproton reservoir. Stable xenon isotopes must be measured during both experimental runs to overlap the measurement data, requiring 4.5 shifts each. Furthermore, 6 shifts per run are needed for stable beam tuning, optimization, and systematic studies to investigate the effect of using different antiproton-ion mixing schemes, trapping times, and beam tunes. We would also like to request 0.5 shifts per run for yield measurements.
Run 1 (UC_x + VD7): 18 shifts

With protons	Requested shifts
Data taking ^{133}Xe, ^{135}Xe, $^{137-144}$Xe	6.5
Yield measurements for $^{142-144}$Xe from UC_x target	0.5
Without protons	Requested shifts
Optimization and systematic studies	6.0
Data taking ^{124}Xe, ^{126}Xe, $^{128-132}$Xe, ^{134}Xe, ^{136}Xe	5.0

Run 2 (LaC_x + VD7): 18 shifts

With protons	Requested shifts
Data taking $^{115-123}$Xe, ^{125}Xe, ^{127}Xe	6.5
Yield measurements for $^{115-117}$Xe	0.5
Without protons	Requested shifts
Optimization and systematic studies	6.0
Data taking ^{124}Xe, ^{126}Xe, $^{128-132}$Xe, ^{134}Xe, ^{136}Xe	5.0

Summary of requested sifts: 36 shifts in 2 runs

A.4 Rate Estimate

Our rate estimate is based on two main objectives: reaching the necessary amount of statistics to achieve the 2% relative measurement uncertainty goal in the shortest possible time while keeping the signal-to-noise rate of better than 10:1 with a maximum signal rate of 100 Hz (limited by front-end electronics).

The background rate Γ_{bckgd} is linearly depending on the density of the co-trapped residual hydrogen molecules $n_{H_2} = 20\,\text{cm}^{-3}$ [24, 10] and the number of antiprotons $N_{\bar{p}}$:

$$\Gamma_{\text{bckgd}} = \lambda_{\text{bckgd}} N_{\bar{p}} = \frac{n_{H_2} N_{\bar{p}}}{5 \times 10^8\,\text{s}\,\text{cm}^{-3}} = \frac{N_{\bar{p}}}{2.5 \cdot 10^7\,\text{s}} = 4 N_{\bar{p}} \times 10^{-8}\,\text{Hz}. \tag{1}$$

The signal rate Γ_{Signal}, on the other hand, depends linearity on both the number of ions N_{ions} and the number of antiprotons at the same time:

$$\Gamma_{\text{Signal}} = \eta \lambda_{\text{Signal}} N_{\text{ions}} = \eta \sigma_{\bar{p}A} \cdot \frac{N_{\bar{p}}}{A} \cdot \sqrt{\frac{2E}{m_N}} \cdot \frac{1}{l} N_{\text{ions}} = 2.8 N_{\bar{p}} N_{\text{ions}} \times 10^{-11}\,\text{Hz}, \tag{2}$$

where $\eta \approx 0.3$ is the expected antiproton-ion overlap, $\sigma_{\bar{p}A} = 10^{-16}\,\text{cm}^2$ [25] is the antiproton-ion annihilation cross-section, $A = 0.25\,\text{cm}^2$ and $l = 5\,\text{cm}$ being the area and length of the

antiproton plasma cloud, respectively, $E = 100\,\mathrm{eV}$ the kinetic energy of the trapped ions with respect to the antiproton plasma, and m_N. With the considered geometries, one can see that the signal-to-noise ratio $\Gamma_{\mathrm{Signal}}/\Gamma_{\mathrm{bckgd}} \approx 7N_{\mathrm{ions}} \times 10^{-4}$ scales only with the number of ions.

Considering now that most isotopes of interest are unstable with a half-life of $t_{1/2}$, then the number of ions during the measurement is given by the annihilation ("signal") rate and their radioactive decay:

$$N_{\mathrm{ions}}(t) = N_{\mathrm{ions,t=0}} \exp\left(-\left(\lambda_{\mathrm{Signal}} + \frac{\ln 2}{t_{1/2}}\right) t\right), \tag{3}$$

where $N_{\mathrm{ions,t=0}}$ is the number of ions at the beginning of an experimental cycle. Similarly, the number of antiprotons over time is given by the annihilation rate with the ions and hydrogen molecules:

$$N_{\bar{\mathrm{p}}}(t) = N_{\bar{\mathrm{p}},t=0} \exp\left(-\left(\lambda_{\mathrm{Signal}} + \lambda_{\mathrm{bckgd}}\right) t\right). \tag{4}$$

Using eq. (3) and eq. (4) inserted in formula (6), one arrives at

$$\Gamma_{\mathrm{Signal}}(t) = \eta \lambda_{\mathrm{Signal}} N_{\mathrm{ions}} = 2.8 N_{\bar{\mathrm{p}}}(t) N_{\mathrm{ions}}(t) \times 10^{-11}\,\mathrm{Hz} \tag{5}$$

$$= 2.8 N_{\bar{\mathrm{p}},t=0} N_{\mathrm{ions,t=0}} \exp\left(-\left(2\lambda_{\mathrm{Signal}} + \lambda_{\mathrm{bckgd}} + \frac{\ln 2}{t_{1/2}}\right) t\right) \times 10^{-11}\,\mathrm{Hz}, \tag{6}$$

For all equations we have stated so far, we have to assume that $\lambda_{\mathrm{Signal}}$ remains constant over the measurement cycle time $\tilde{t}$ as $\lambda_{\mathrm{Signal}}$ depends on the available number of antiprotons and ions. In a simple approach, this can be achieved by keeping $N_{\bar{\mathrm{p}},t=0} \gg N_{\mathrm{ions,t=0}}$ at the start of the cycle, meaning for short-lived isotopes, the cycle time has to be as short as possible to replenish the interaction region with "new" ions.

We motivate the number of antiproton-ion annihilations $N_{\bar{\mathrm{p}}A}$ to reach our precision goal as follows: due to the geometry of the trap, pions will be correctly detected with an 80% chance. This leads to a broadening of the measured pion-charge-sum (Σ) distribution. The probability $p_{\bar{\mathrm{p}}\mathrm{p}}(\Sigma = 0)$ to measure $\Sigma = 0$ in an antiproton-proton annihilation is no longer equal to 1 (as one would expect from charge-conservation) but follows a distribution (see Tab. 4). The uncertainty is calculated as

$$\Delta p = \sqrt{p \cdot \frac{(1-p)}{N}}. \tag{7}$$

The probability of measuring a certain Σ after an antiproton-isotope annihilation is

$$p_{\bar{\mathrm{p}}A}(\Sigma) = p_{\bar{\mathrm{p}}\mathrm{p}}(\Sigma) \cdot \frac{1}{{}^{n}/_{p} + 1} + p_{\bar{\mathrm{p}}\mathrm{n}}(\Sigma) \cdot \frac{{}^{n}/_{p}}{{}^{n}/_{p} + 1} \tag{8}$$

$$\Leftrightarrow {}^{n}/_{p} = \frac{p_{\bar{\mathrm{p}}A}(\Sigma) - p_{\bar{\mathrm{p}}\mathrm{p}}(\Sigma)}{p_{\bar{\mathrm{p}}\mathrm{n}}(\Sigma) - p_{\bar{\mathrm{p}}A}(\Sigma)}, \tag{9}$$

with $p_{\bar{\mathrm{p}}i}(\Sigma)$ given in Tab. 4 and $p_{\bar{\mathrm{p}}A}(\Sigma)$ measured by the experiment. The statistical uncertainty is given by

$$\Delta {}^{n}/_{p} = \frac{\left|p_{\bar{\mathrm{p}}\mathrm{n}} - p_{\bar{\mathrm{p}}\mathrm{p}}\right|}{\left(p_{\bar{\mathrm{p}}\mathrm{n}} - p_{\bar{\mathrm{p}}A}\right)^2} \cdot \Delta p_{\bar{\mathrm{p}}A}, \tag{10}$$

Table 4: The probability to measure a certain pion charge-sum Σ after an antiproton annihilation with a proton $p_{\bar{p}p}$ and a neutron $p_{\bar{p}n}$. The uncertainties result from a simulation with $N = 10^4$ annihilations and can be improved through larger statistics.

Σ	$p_{\bar{p}p}$	$\Delta p_{\bar{p}p}$	$p_{\bar{p}n}$	$\Delta p_{\bar{p}n}$
-3	0.0000	0.0000	0.0005	0.0002
-2	0.0162	0.0013	0.0820	0.0027
-1	0.1765	0.0038	0.6490	0.0048
0	0.5692	0.0050	0.2425	0.0043
1	0.2182	0.0041	0.0256	0.0016
2	0.0199	0.0014	0.0004	0.0002
3	0.0000	0.0000	0.0000	0.0000

with $\Delta p_{\bar{p}A}$ following Eq. 7. To achieve a relative uncertainty of 2%, the number of annihilation $N_{\bar{p}A}$ is

$$\frac{\Delta n/p}{n/p} \stackrel{!}{=} 0.02 \tag{11}$$

$$= \frac{\left|p_{\bar{p}n} - p_{\bar{p}p}\right|}{\left(p_{\bar{p}n} - p_{\bar{p}A}\right)\left(p_{\bar{p}A} - p_{\bar{p}p}\right)} \cdot \Delta p_{\bar{p}A} \tag{12}$$

$$= \frac{\left|p_{\bar{p}n} - p_{\bar{p}p}\right|}{\left(p_{\bar{p}n} - p_{\bar{p}A}\right)\left(p_{\bar{p}A} - p_{\bar{p}p}\right)} \cdot \sqrt{p_{\bar{p}A} \cdot \frac{\left(1 - p_{\bar{p}A}\right)}{N_{\bar{p}A}}} \tag{13}$$

$$\Leftrightarrow N_{\bar{p}A} = \frac{1}{\frac{\Delta n/p}{n/p}}^2 \cdot \frac{p_{\bar{p}A}(1 - p_{\bar{p}A})(p_{\bar{p}p} - p_{\bar{p}n})^2}{(p_{\bar{p}p} - p_{\bar{p}A})^2 (p_{\bar{p}n} - p_{\bar{p}A})^2}. \tag{14}$$

Over a broad range of neutron-to-proton ratios n/p, larger than the range covered by the xenon isotopes, $N_{\bar{p}A} \approx 10^5$ is sufficient to reach a relative uncertainty of $\frac{\Delta n/p}{n/p} = 0.02$.
To summarize, we list the three conditions:

1. Signal to noise ratio $7 N_{ions} \times 10^{-4} > 10$
2. Overall signal rate $2.8 N_{\bar{p}} N_{\text{ions}} \times 10^{-11}\,\text{Hz} + 4 N_{\bar{p}} \times 10^{-8}\,\text{Hz} \leq 100\,\text{Hz}$
3. Number of annihilations $N_{\bar{p}A} \approx 10^5$

To guarantee the availability of ions in the interaction region, we need the RC6 RFQ-cb or ISCOOL RFQ-cb to deliver $N_{\text{ions,t=0}} = 10^5$ ions per bunch every $\tilde{t} = 2.4\,\text{s}$, assuming every other cycle in the Proton Synchrotron Booster super cycle is available and the fast-released xenon isotopes are collected in either RFQ-cb after proton impact for 500 ms to 1 s, depending on their half-life. Estimating losses in the RFQ-cb due to charge exchange with the buffer gas for cooling times up to 1 s to be less than 10% [26], and an overall conservative trapping efficiency of 20%, the lower yield limit is in the order of 5×10^5 per µC.

Assuming a realistic experimental cycle time of $\tilde{t} = 2.4\,\text{s}$, a desired number of antiproton-ion annihilations $N_{\bar{p}A} = 10^5$ we estimate the necessary measurement time by

integrating over the rate

$$T = \frac{N_{\bar{\mathrm{p}}A} \cdot \tilde{t}}{\int_0^{\tilde{t}} \Gamma_{\mathrm{Signal}}(t)\mathrm{d}t}, \tag{15}$$

where $N_{\bar{\mathrm{p}}A}$ is the number of antiproton-ion annihilation events.

For the shortest-living isotope on the proposed list, with $t_{1/2} = 388\,\mathrm{ms}$ for ^{144}Xe, the effective measurement time is 8.6 h using $N_{\bar{\mathrm{p}}} = 5\times10^6$, $N_{\mathrm{ions}} = 10^5$, and $N_{\bar{\mathrm{p}}A} = 10^5$, which yields an effective signal rate of 7.75 per cycle of 2.4 s, with a signal-to-noise ratio of ≈ 70 at $t = 0$. Due to the rapid decay of the signal rate due to the nuclear decay, the signal-to-noise ratio drops below 10 after only three half-lives (1.2 s), the effective data collection time can only be 1.2 s, corresponding to 7 counts yielding 9.6 h of measurement time. When radioactive decay does not play a role, i.e. when $t_{1/2} \gg \tilde{t}$, then the signal rate can be seen as constant (still assuming $N_{\bar{\mathrm{p}}} \gg N_{\mathrm{ions}}$). In the cases of isotopes with $t_{1/2} > 5\,\mathrm{s}$, the measurement time is reduced to $< 5.0\,\mathrm{h}$, taking into account that too large a number of N_{ions} would exceed the rate limit of the data acquisition, setting a lower limit.

A.5 Expected safety hazards at the new RC7 beamline

- Design and manufacturing
  - ☒ Consists of standard equipment supplied by a manufacturer
  - ☐ CERN/collaboration responsible for the design and/or manufacturing
- Radioactive sources: none
- Collections: none
- Describe the hazards generated by the experiment:

Domain	Hazards/Hazardous Activities		Description
Mechanical Safety	Pressure	☐	
	Vacuum	☒	10^{-11} mbar
	Machine tools	☐	
	Mechanical energy (moving parts)	☐	
	Hot/Cold surfaces	☐	
Cryogenic Safety	Cryogenic fluid	☐	
Electrical Safety	Electrical equipment and installations	☐	
	High Voltage equipment	☒	Up to 30kV on the pulsed drift tube, up to 3.5kV on other ion optical elements
Chemical Safety	CMR (carcinogens, mutagens and toxic to reproduction)	☐	
	Toxic/Irritant	☐	
	Corrosive	☐	
	Oxidizing	☐	
	Flammable/Potentially explosive atmospheres	☐	

	Dangerous for the environment	☐	
Non-ionizing radiation Safety	Laser	☐	
	UV light	☐	
	Magnetic field	☒	Static 4T
Workplace	Excessive noise	☐	
	Working outside normal working hours	☒	Shiftwork during scheduled experiment
	Working at height (climbing platforms, etc.)	☐	
	Outdoor activities	☐	
Fire Safety	Ignition sources	☐	
	Combustible Materials	☐	
	Hot Work (e.g. welding, grinding)	☐	
Other hazards	Antiprotons	☒	Can produce ionizing radiation upon annihilation